

Article

Characterization and Evaluation of the Antioxidant, Antidiabetic, Anti-Inflammatory, and Cytotoxic Activities of Silver Nanoparticles Synthesized Using *Brachychiton populneus* Leaf Extract

Muhammad Naveed ^{1,*}, Hira Batool ¹, Shafiq ur Rehman ², Aneela Javed ³, Syeda Izma Makhdoom ¹, Tariq Aziz ^{4,*}, Amal A. Mohamed ^{5,6}, Manal Y. Sameeh ⁵, Mashael W. Alruways ⁷, Anas S. Dablood ⁸, Abdulraheem Ali Almalki ⁹, Abdulhakeem S. Alamri ⁹, and Majid Alhomrani ⁹

¹ Department of Biotechnology, Faculty of Life Sciences, University of Central Punjab, Lahore 54590, Pakistan; hirabatool337@gmail.com (H.B.); izmamakhdoom@gmail.com (S.I.M.)

² Department of Basic and Applied Chemistry, Faculty of Sciences, University of Central Punjab, Lahore 54000, Pakistan; shafiq.rehman@ucp.edu.pk

³ Department of Healthcare Biotechnology, Atta-ur-Rahman School of Applied Biosciences (ASAB), National University of Science and Technology (NUST), Islamabad 44000, Pakistan; javedaneela19@asab.nust.edu.pk

⁴ Pak-Austria Fachhochschule, Institute of Applied Sciences and Technology, Mang, KPK, Haripur 22621, Pakistan

⁵ Chemistry Department, Al-Leith University College, Umm Al-Qura University, Makkah 24831, Saudi Arabia; aaaydeyaa@uqu.edu.sa (A.A.M.); myassemih@uqu.edu.sa (M.Y.S.)

⁶ Plant Biochemistry Department, National Research Centre, Cairo 12622, Egypt

⁷ Department of Clinical Laboratory Sciences, College of Applied Medical Sciences, Shaqra University, Shaqra 15273, Saudi Arabia; m.alruways@su.edu.sa

⁸ Department of Public Health, Health Sciences College Al-Leith, Umm Al-Qura University, Makkah al-Mukarramah 24382, Saudi Arabia; asdablood@uqu.edu.sa

⁹ Department of Clinical Laboratory Sciences, The Faculty of Applied Medical Sciences, Taif University, P.O. Box 11099, Taif 21944, Saudi Arabia; almalki@tu.edu.sa (A.A.A.); a.alamri@tu.edu.sa (A.S.A.); m.alhomrani@tu.edu.sa (M.A.)

* Correspondence: dr.naveed@ucp.edu.pk (M.N.); iwocdkd@gmail.com (T.A.)



Citation: Naveed, M.; Batool, H.; Rehman, S.u.; Javed, A.; Makhdoom, S.I.; Aziz, T.; Mohamed, A.A.; Sameeh, M.Y.; Alruways, M.W.; Dablood, A.S.; et al. Characterization and Evaluation of the Antioxidant, Antidiabetic, Anti-Inflammatory, and Cytotoxic Activities of Silver Nanoparticles Synthesized Using *Brachychiton populneus* Leaf Extract. *Processes* **2022**, *10*, 1521. <https://doi.org/10.3390/pr10081521>

Academic Editors: Luigi Menghini and Claudio Ferrante

Received: 8 July 2022

Accepted: 26 July 2022

Published: 2 August 2022

Publisher's Note: MDPI stays neutral with regard to jurisdictional claims in published maps and institutional affiliations.



Copyright: © 2022 by the authors. Licensee MDPI, Basel, Switzerland. This article is an open access article distributed under the terms and conditions of the Creative Commons Attribution (CC BY) license (<https://creativecommons.org/licenses/by/4.0/>).

Abstract: Bionanotechnology is the combination of biotechnology and nanotechnology for the development of biosynthetic and environmentally friendly nanomaterial synthesis technology. The presented research work adopted a reliable and environmentally sustainable approach to manufacturing silver nanoparticles from *Brachychiton populneus* (BP-AgNPs) leaf extract in aqueous medium. The *Brachychiton populneus*-derived silver nanoparticles were characterized by UV–Vis spectroscopy, Fourier-transform infrared spectroscopy (FTIR), scanning electron microscopy (SEM), and energy dispersive X-ray analysis (EDX). In addition, the antioxidant, anti-inflammatory, antidiabetic, and cytotoxic activities of AgNPs were brought to light. The synthesis of BP-AgNPs was verified at 453 nm wavelength by UV–Vis spectrum. FTIR analysis revealed that synthesis, stability, and capping of AgNPs depend on functional groups such as alkane, alkene, nitro, fluoro, phenol, alcoholic, and flavones, present in plant extract. The SEM analysis revealed evenly distributed cubical-shaped nanoparticles. The average diameter of AgNPs was 12 nm calculated from SEM image through ImageJ software. EDX spectrum confirmed the presence of Ag at 3 keV and other trace elements such as oxygen and chlorine. The biosynthesized silver nanoparticles exhibited proven antioxidant (DPPH assay), antidiabetic (alpha amylase assay), anti-inflammatory (albumin denaturation assay), and cytotoxic (MTT assay) potential against U87 and HEK293 cell lines in comparison to standard drugs. In these assays, BP-AgNPs exhibited inhibition in a concentration-dependent manner and had lower IC₅₀ values compared to standards. All these outcomes suggest that silver nanoparticles work as a beneficial biological agent. The salient features of biosynthesized silver nanoparticles propose their effective applications in the biomedical domain in the future.

Keywords: *Brachychiton populneus*; green synthesis; silver nanoparticles; antioxidant; antidiabetic; anti-inflammatory activity

1. Introduction

Nanotechnology and nanoscience have undergone a remarkable revolution in the current century by exploring this mysterious area of research. A lecture entitled “There’s plenty of room at the bottom” is credited with discovering nanotechnology. Nanotechnology is implemented in all disciplines of science including engineering, information technology, material science, and life science, along with clarifying astonishing facts regarding human health, specifically in cancer treatment. The array of atoms on a 1–100 nm scale, nanodevices, systems, and structures makes them feasible in the research area [1]. The formation of nanostructures is based on two strategies: the bottom-up and top-down synthesis methods. The top-down strategy is used to convert massive substances into nanoparticles. The bottom-up approach creates nanostructures based on atom by atom or molecule by molecule organization using chemical and physical processes [2]. Nanoparticles are synthesized by chemical, physical, and biological methods. In biological methods, bacteria, yeast, fungi, algae, and plants are the key factors used to synthesize metallic nanoparticles [3].

Plant-based synthesis of nanoparticles depends on the presence of bioactive metabolites such as polysaccharides, amino acids, aldehydes, flavones, alkaloids, proteins, phenolics, saponins, terpenoids, tannins, ketones, and vitamins in plants. These are the metabolites that serve as reducing and capping agents in nanoparticle formation [4]. Silver nanoparticles (AgNPs) are highly significant and captivating nano-formations among various noble metal-based nanoparticles that are administered in many biological pathways to overcome critical illnesses. Green synthesis of silver nanoparticles using plant extracts has become the most encouraging method due to its low cost and its being biologically compatible, environment-friendly, and safe to handle. Silver nanoparticles reveal excellent biological properties, such as antimicrobial, anti-inflammatory, antidiabetic, antioxidant, anticancer, and antiviral activities [5,6]. AgNPs act as biosensors because of their surface plasmon resonance capabilities. These sensors target contaminants such as heavy metals, insecticides, etc., that are released into the environment [7].

Brachychiton populneus, commonly called the Kurrajong or Bottelboom, belongs to the *Sterculaceae* family. It is a medium-sized ornamental tree native to Australia and cultivated in other countries. It grows to approximately 20 m tall and has a somewhat small trunk and a densely foliated pinnacle. Active ingredients, such as terpenes, sterols, flavonoids, alkaloids, and coumarins, are some of the synthetic chemicals found in species of this family that have antioxidant, bactericidal, anti-inflammatory, and antidiabetic activities [8–10].

Silver nanoparticles have been widely used in domestic items, public health care, ambient atmosphere, and medical management. AgNPs had practical bactericidal ability against the microorganisms studied, with the highest bactericidal activity being against *Staphylococcus aureus* and *Bacillus subtilis* [11]. Anti-inflammatory properties of silver nanoparticles were also reported. Vascular Endothelial Growth Factor, (HIF)-1 α activity is inhibited, limiting mucin hypersecretion, decreasing pro-inflammatory mediators released by silver nanoparticles and, consequently, regulating gene functioning to avoid infections [12]. Cancer is a deadly disease which affects one in every three people at some point in their lives. Various chemopreventive drugs are now approved for the management of cancer cases, but they come with a variety of harmful impacts, and administering antitumor medications intramuscularly is an inadequate technique [13]. Plant organs-assisted silver nanoparticle production has been demonstrated on tumor cell lines in the human respiratory system [14,15].

Green synthesized metal nanoparticles have an incredible aptitude against diabetes and regulate the functioning of diabetes by α -amylase release from pancreases, colonic,

a-glucosidase, insulin levels, glycemic absorption, and other histochemistry characteristics during in-vivo and in vitro studies [16]. Metal-based nanoparticles were discovered to have antioxidant capabilities, scavenging free radicals and lowering reactive oxygen species (ROS) production. The exact chemical pathways that determine metal nanoparticles' antioxidant properties are yet unknown. The large surface area and electrical configuration act as catalysts for oxidant-reduction reaction characteristics, and oxygen point defects in these NPs are thought to be responsible for their antioxidant capacity [17–20]. Therapy with nano-based developed medicines, in comparison to essential medication, may be a potent clinical alternative for people with significant disorders due to such features. The current work reports an unprecedented one-step, cost-effective approach for AgNPs production from *Brachychiton populneus* plant leaf extract at room temperature, which shows distinctive biological properties, such as anti-inflammatory, antidiabetic, antioxidant, and anti-cancer, has no negative impacts and precisely addresses the intended organoids.

2. Materials and Methods

2.1. Collection of *Brachychiton Populneus* Leaves

The leaves of the plant *Brachychiton populneus* were collected from Lawrence Garden, Lahore.

2.2. Preparation of Leaves Extracts

To eliminate contaminants, the gathered leaves were rigorously cleaned with distilled water. The leaves were then dried for three hours at 55 °C in a hot air oven. Dried leaves were pulverized in an electric blender to create a fine powder. Five grams of leaf powder was then placed in a beaker which was then filled with 600 mL of distilled water. At 80 °C, the beaker was placed on a magnetic stirrer and continuously stirred at 1500 rpm for 45 min. After that, the extract was filtered in a flask using Whatman No. 1 filter paper and stored in a refrigerator at 4 °C for further use.

2.3. Formation of Silver Nitrate (AgNO_3) Dilutions

The silver nitrate solution was prepared by dissolving crystalline AgNO_3 in distilled water to make a 1 M stock solution. Then, from this stock, sequential dilutions of 5 mM, 10 mM, 15 mM, 20 mM, and 25 mM were prepared to fabricate silver nanoparticles.

2.4. Leaf Extract-Mediated BP-AgNPs Synthesis

For nanoparticle synthesis, the prepared silver nitrate solution and plant extract were mixed together in a 1:9 *v/v* ratio to make a final volume of 200 mL in a reagent bottle. The bottle was tightly capped and covered with aluminum foil. The reaction mixture was incubated until the yellow color turned brown/black. After color change, the solution was centrifuged at 4000 rpm for 30 min and the supernatant was discarded. This step was repeated three times with vigorous washing with distilled water to remove unwanted components from the pellet. The pellet was then dissolved in distilled water and dried in a hot air oven at 4 °C overnight. The obtained crystalline particles were further used for characterization.

2.5. Characterization of Silver Nanoparticles

2.5.1. Ultraviolet-Visible Spectrophotometer

UV-visible spectroscopy is a verification technique for the formation of nanoparticles. The spectra were recorded on the double beam spectrophotometer in the range of 300–700 nm to ensure the fabrication of silver nanoparticles [21]. For analysis, 3 mL of silver nanoparticles was poured into a glass cuvette, and distilled water was utilized as a blank.

2.5.2. Fourier-Transform Infrared (FTIR) Spectroscopy

The Fourier-transform infrared (FTIR) spectroscopy is the most extensively practiced technique. This technique is based on infrared radiation that moves across the substances to be analyzed. The substance absorbs some energy rays and many of them will be passed on from substances. As a result, the absorption spectra reveal a detailed pattern of the studied material's chemical composition [21]. In the current study, Fourier-transform infrared spectroscopy was used to explore the functional composition of the nano-formation in the region of $4000\text{--}650\text{ cm}^{-1}$.

2.5.3. Scanning Electron Microscopy (SEM)

The Nova Nano FE-SEM 450 (FEI) scanning electron microscope examined the samples for topographical and compositional information. The DBS and LVD installed on the lens provided high-quality data collection and optimized the profile. With a resolution of 1.4 nm at 1 kV (TLD-SE) and 1 nm at 15 kV, beam landing energy may be reduced from 30 keV to 50 keV (TLD-SE). Prior to SEM analysis, the whole sample was camouflaged with gold.

2.5.4. Energy Dispersive X-ray Analysis (EDX)

The trace elemental composition of *BP-AgNPs* was analyzed by EDX analyzer attached with SEM machine Nova Nano FE-SEM 450.

2.6. In Vitro Biological Screening of Silver Nanoparticles

2.6.1. Antioxidant Activity of Silver Nanoparticles (DPPH ASSAY)

To evaluate the scavenging capacity of DPPH, an assay was performed according to the reported method [22]. *BP-AgNPs* ($10\text{--}70\text{ }\mu\text{g/mL}$) in distilled water were mixed with 1 mL of methanol solution that contained DPPH radicals (0.1 mM). Before measuring the absorbance at 517 nm against a blank, the mixture was violently mixed and allowed to stand for 30 min in the dark. Furthermore, using the given formula, the scavenging ability was estimated at:

$$\text{Percentage Inhibition} = [(A_c - A_s)/A_s] \times 100$$

where A_c represents the absorbance of the control reaction, which contains all components except the test component, and as such, represents the absorbance of the synthesized compounds.

2.6.2. Inhibition of Enzymatic Activity of α -Amylase by *BP-AgNPs*

The antidiabetic activity was assessed through an alpha-amylase assay [23]. Different concentrations of *BP-AgNPs* ($25\text{--}125\text{ }\mu\text{g/mL}$) were prepared in ethanol. In separate sterile tubes, reaction mixture was prepared by mixing 250 μL of *AgNPs* solution, 200 μL of 2% starch solution, 250 μL of sodium phosphate buffer (pH 6.9), and 200 μL of 1 U/mL alpha-amylase solution, and the tubes were then vortexed. The mixture was incubated at room temperature for several minutes. After incubation, 450 μL of dinitro salicylic acid was added to all tubes to terminate the reaction. The tubes were then placed into a boiling water bath for 5 min and a change in color intensity was observed. A control reading was taken without a sample and absorption was noted at 540 nm. The standard drug was treated similarly to the test sample. Amylase inhibition was calculated using the following equation:

$$\text{Percentage Inhibition} = [(A_c - A_s)/A_s] \times 100$$

2.6.3. Inhibition of Protein Denaturation by *BP-AgNPs*

Albumin denaturation inhibition assay was employed to study the possible mechanisms for the anti-inflammatory impact of *BP-AgNPs*, according to previously published papers with slight modifications [24]. To conduct the assay, an albumin solution was pre-

pared using a hen's egg, along with various quantities of silver nanoparticles ranging from 20 to 100 µg/mL. Then, in separate sterile tubes, 300 µL of albumin solution and 400 µL of silver nanoparticles were mixed. The reaction mixture was then adjusted to pH 6.4 using phosphate buffer. To elicit the denaturation of egg albumin, the reaction mixture was incubated at room temperature for 20 min before being heated in a water bath for 15 min at 65 °C. After that, the tubes were cooled, and the absorbance was measured using a UV visible spectrophotometer at 660 nm. As a blank, distilled water was utilized. Diclofenac sodium was used as a standard drug and was processed similarly to the nanoparticles sample. As a control, DMSO was utilized. The reaction was repeated three times and an average taken. The percentage inhibition was estimated using the following formula,

$$\text{Percentage Inhibition} = [(A_c - A_s)/A_s] \times 100$$

2.6.4. Cytotoxic Activity of AgNPs on Cell Lines (MTT Assay)

Culturing of Cell Lines

Cell cytotoxicity experimentations were performed on the adherent cell lines, U87-MG and HEK. The cells were cultured in T-25 flasks in pre-warmed complete DMEM media. The media was supplemented with 10% Fetal Bovine Serum and 1% of Penstrep was also added to the cell culture medium to prevent contamination by micro-organisms. The culture flasks were kept in a humidified water-jacketed incubator at 37 °C temperature and 5% CO₂ to allow U87-MG and HEK cell growth.

Assay for % Cell Viability

Assays were performed upon the samples with exposures of 24 and 48 h, after which the assay procedures were carried out. Various concentrations of the samples (250 µg, 100 µg, 50 µg, 10 µg, 1 µg) were prepared by dissolving the required amount in double distilled, filtered PBS through thorough sonication. The assay was performed as follows:

Day 1: U87 and HEK cells (100 µL/well) were plated at a density of 1.0×10^3 cells/mL into 96 healthy plates and were incubated in a CO₂ incubator for 24 h to adhere.

Day 2: When cells were seeded, then 100 µL of sample dilutions at different concentrations (250 µg, 100 µg, 50 µg, 10 µg, 1 µg) were added to the adhered cells in triplicates. These were allowed to produce their effect on the cells for another 24 and 48 h in an incubated environment.

Day 3 and 4: After 24 or 48 h, 15 µL of filter sterilized MTT (5 mg/mL in PBS) was added to the microtiter wells. The plates were again incubated for 3 h for the reduction reaction to take place.

After a 3-h incubation with MTT, the wells were carefully emptied through pipetting then 100 µL of sterile DMSO was added to the wells which were then given 30 min incubation at 37 °C to precipitate the purple-colored insoluble crystals of formazan that were entrapped in the viable cells. After this, the absorbance of formazan was measured at 550 nm with a spectrophotometric microplate reader.

2.7. Statistical Analysis

All assays were performed in triplicate, and through SPSS software version 2020, statistical analysis was performed. By running one-way ANOVA (mean ± SD) was calculated at ($p < 0.05$) significance level.

3. Results

3.1. Phyto-Mediated Reduction of Ag⁺ Ions to Ag⁰

The leaf extract upon reaction with 25 mM AgNO₃ solution reduced Ag ions and as a result, the color of the solution turned from yellow to blackish brown (Figure 1).



Figure 1. Indication of color change after reduction of AgNO_3 .

3.2. Characterization of Silver Nanoparticles

3.2.1. UV-Visible Spectrophotometric Analysis

The UV-Vis spectrum was recorded in the range of 300–700 nm wavelength. In UV-visible absorption spectra, the colloidal solution of silver nanoparticles indicated a surface plasmonic peak at 453 nm due to SPR, which confirms the synthesis and stability of silver nanoparticles (Figure 2).

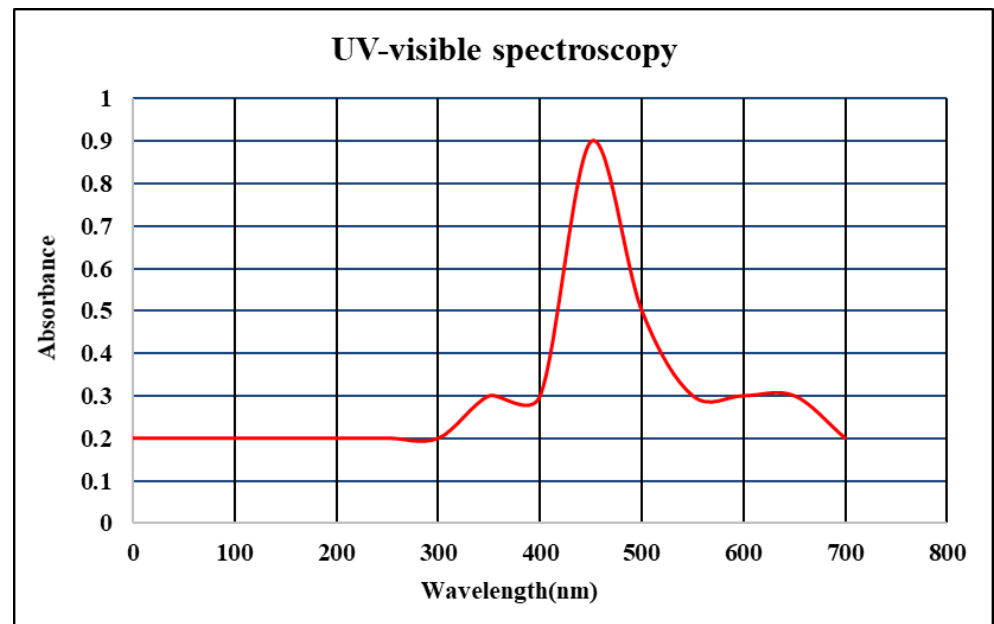


Figure 2. Confirmation of silver nanoparticles synthesis by UV-visible spectroscopy.

3.2.2. Fourier-Transform Infrared Spectroscopy (FTIR)

The FT-IR spectra of synthesized silver nanoparticles (*BP-AgNPs*) were investigated, and the outcomes are shown in the figure. The absorption peaks confirmed the existence of functional groups in the plant extract that are responsible for the formation of silver

nanoparticles. The peak at 2924.6 cm^{-1} was attributed to (O–H) and (C–H) stretching vibrations, which were composed of an alkane group and an alcohol compound. The two peaks at 1508.2 cm^{-1} and 1522.6 cm^{-1} were accredited to (N–O) stretching, and the one at 1231.4 was attributed to (C–N) stretching vibrations of the nitro compound. Conjugated alkene, amine group, and a cyclic alkene with (C=C) stretching and (N–H) bending were confirmed due to one peak at 1625 cm^{-1} and the other at 1638 cm^{-1} . The absorption band at 1313 cm^{-1} indicates (O–H) bending and (S–O) stretching vibrations, which confirm the presence of phenol and sulfone compounds. A halo compound with (C–Cl) stretching vibrations was verified by an absorption band at 1041.8 cm^{-1} . In comparison, the presence of a fluoro compound with (C–F) stretching vibrations was highlighted by an absorption band at 779 cm^{-1} . All these functional groups exhibit tremendous participation in stabilizing silver nanoparticles (Figure 3).

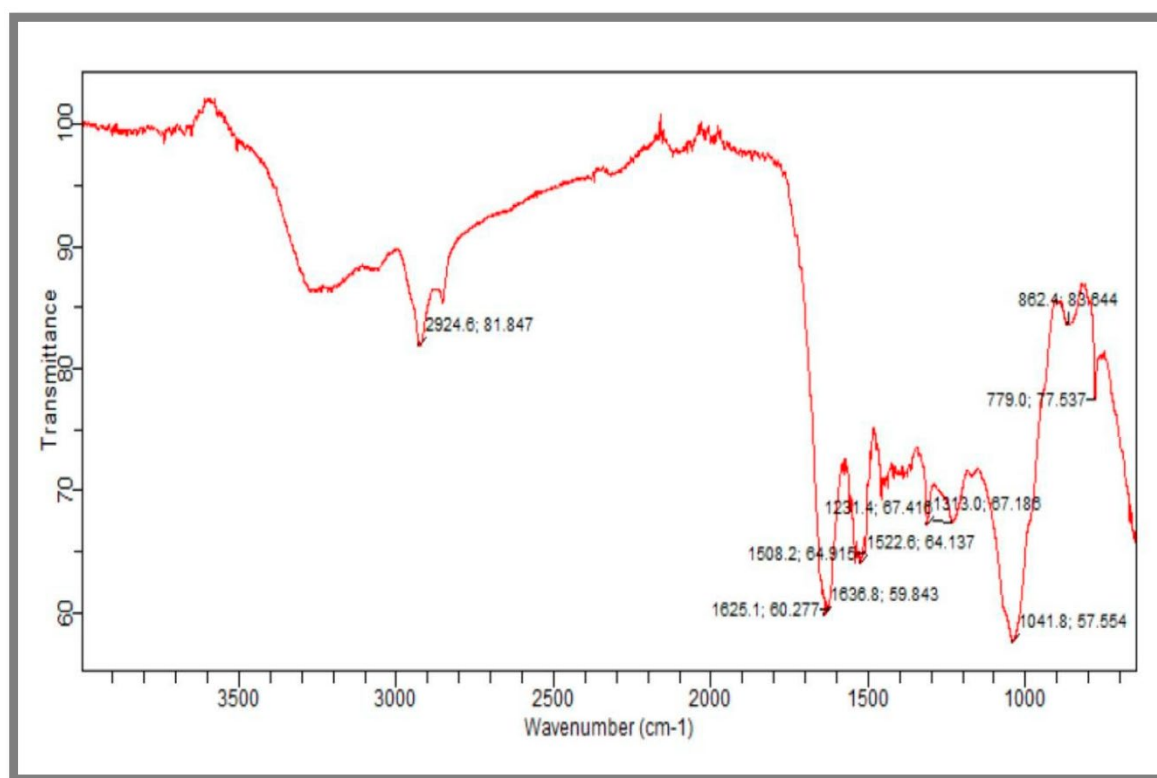


Figure 3. Fourier-transform infrared spectroscopy of synthesized nanoparticles to analyze functional groups responsible for the reduction of Ag ions.

3.2.3. Scanning Electron Microscopy (SEM)

Scanning electron microscopy of silver nanoparticles (BP-AgNPs) demonstrates that particles are evenly distributed and cubical in shape (Figure 4). The average size of crystalline nanoparticles calculated using ImageJ software (J904 BETA) was 15 nm (Figure 5).

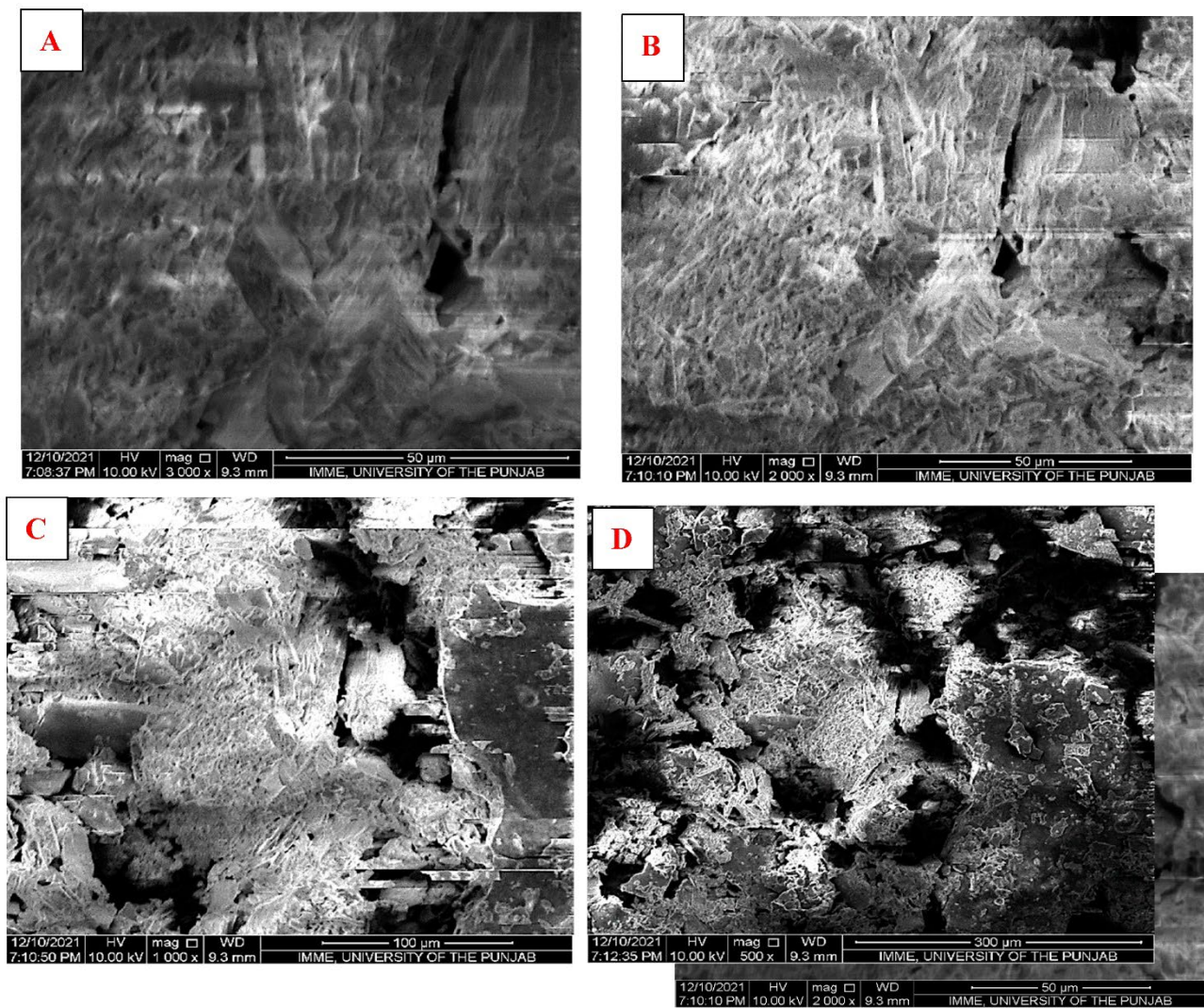


Figure 4. SEM micrograph of silver nanoparticles (BP-AgNPs) 3000× (A), 2000× (B), 1000× (C) and 500× (D) magnification.

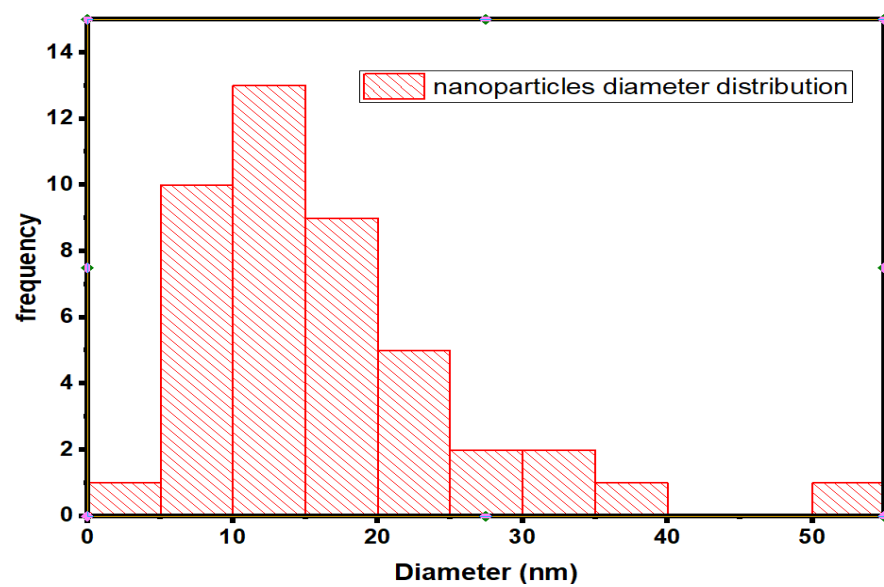


Figure 5. Histogram for nanoparticle diameter distribution.

3.2.4. Energy Dispersive X-ray Analysis (EDX)

EDX analysis revealed the elemental composition of synthesized nanoparticles. These metallic silver nanoparticles express a sharp peak at 3 keV due to their SPR, which confirms the presence of silver ions and other elements, carbon, oxygen, and chlorine, act as reducing and capping agents (Figure 6). Analysis shows the absence of nitrogen that ensures complete reduction of AgNO_3 into silver ions, and no other trace ions are present in nanoparticles (Table 1).

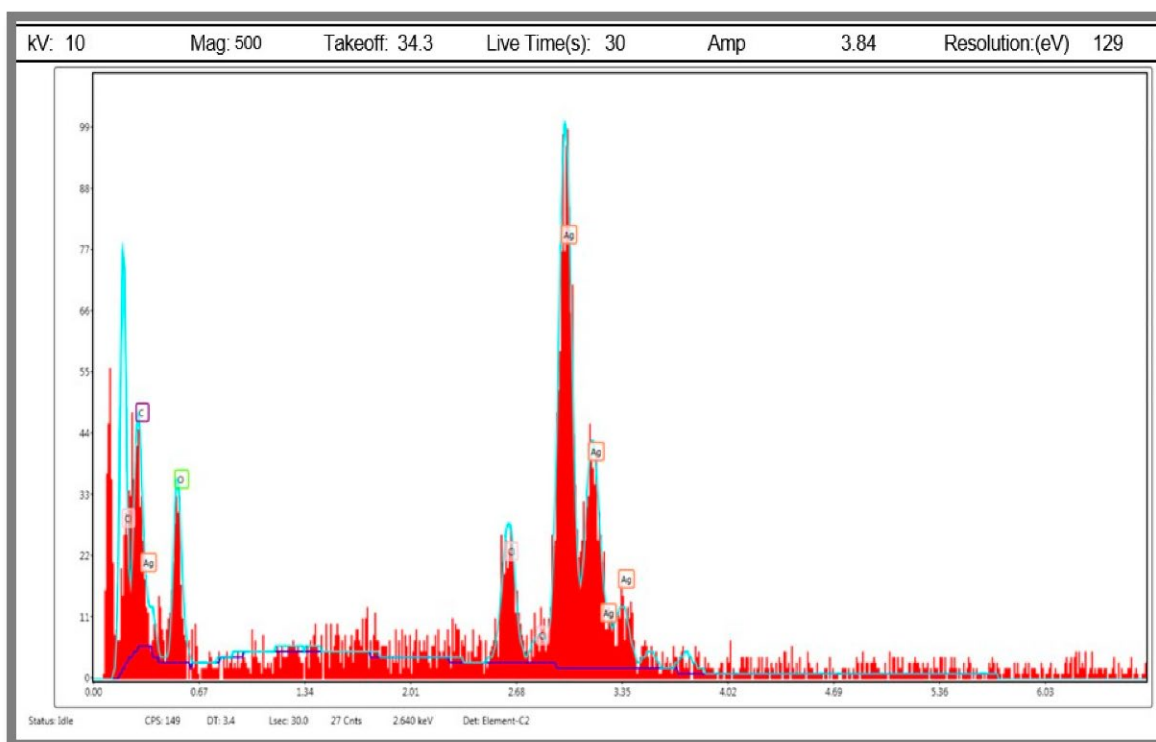


Figure 6. The EDX spectrum of silver nanoparticles (BP-AgNPs) depicts an Ag peak between 2–3 KeV.

Table 1. Elemental composition of synthesized silver nanoparticles.

Element	Weight %	Atomic %	Net Int.
C K	4.56	20.13	6.02
O K	9.13	30.3	6.11
ClK	7.05	10.56	7.44
AgL	79.26	39.01	33.36

3.3. In vitro Biological Screening of *Brachycton Populneus* Mediated AgNPs

3.3.1. Antioxidant Activity Silver Nanoparticles (DPPH Assay)

The radical scavenging activity of biosynthesized silver nanoparticles from *Brachycton populneus* leaf extract was observed by the change in color of DPPH solution containing nanoparticles. The change in color from violet to light yellow indicates that synthesized nanoparticles have antioxidant potential, and this was further quantified using a spectrophotometer. The BP-AgNPs revealed more inhibition (23 to 95%) than standard ascorbic acid (13 to 79%) in a dose-dependent manner at the same concentrations (10–70 $\mu\text{g}/\text{mL}$). The half-maximal inhibitory concentration IC_{50} values for BP-AgNPs and ascorbic acid is 33.85 $\mu\text{g}/\text{mL}$ and 50 $\mu\text{g}/\text{mL}$ respectively, which shows that AgNPs have higher antioxidant potency than ascorbic acid as shown in Figure 7 and Table 2.

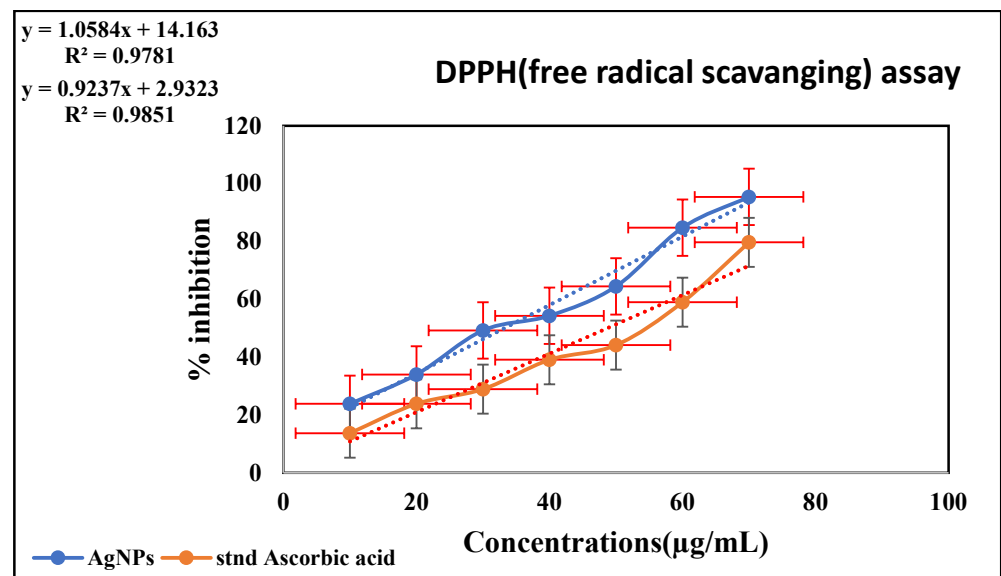


Figure 7. Antioxidant activity in a dose-dependent manner of biosynthesized BP-AgNPs from *Brachychiton populneus* leaf extract. Ascorbic acid is treated as a positive control. Experiments performed in triplicates and using one-way ANOVA indicate that all values are significant ($p < 0.05$).

Table 2. Values represented in (Mean \pm SD) and significant level ($p < 0.05$), through one-way ANOVA of DPPH assay.

Concentrations (µg/mL)	Mean \pm SD (AgNPs)	Mean \pm SD (Ascorbic Acid)
10	0.15 \pm 0.01	0.17 \pm 0.02
20	0.13 \pm 0.01	0.15 \pm 0.01
30	0.10 \pm 0.02	0.14 \pm 0.03
40	0.09 \pm 0.01	0.12 \pm 0.02
50	0.07 \pm 0.02	0.11 \pm 0.01
60	0.03 \pm 0.01	0.08 \pm 0.03
70	0.009 \pm 0.00	0.08 \pm 0.01

3.3.2. Inhibition of Enzymatic Activity of α -Amylase by BP-AgNPs

In the alpha-amylase assay, the less intense red color declared synthesized BP-AgNPs as an alpha-amylase enzyme inhibitor. The activity is demonstrated in a dose-dependent way as an increase in concentration (25–125 µg/mL) increases the percentage inhibition (32–80%). The maximum inhibition revealed by AgNPs was 80%, and the standard drug acarbose exhibited 60% inhibition at the same concentration (125 µg/mL). The IC_{50} values calculated from the regression equation for BP-AgNPs and Acarbose are (67 µg/mL) and (110 µg/mL), respectively. The results illustrate the dominant capability of biosynthesized AgNPs as an antidiabetic agent over reference drugs (Figure 8) with significant values shown in Table 3.

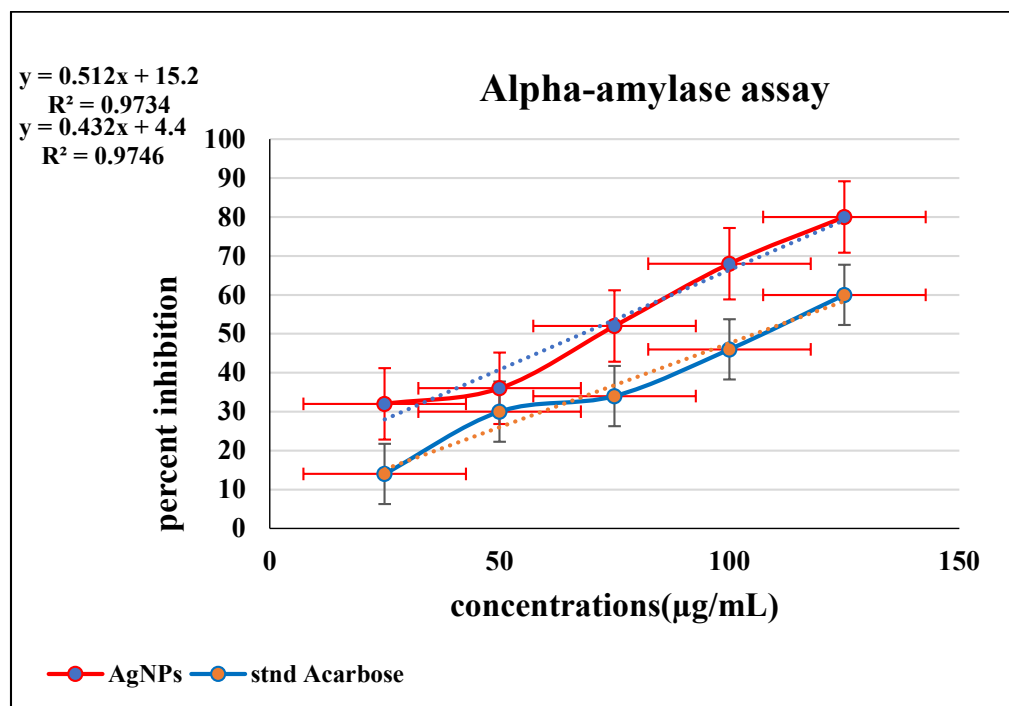


Figure 8. Shows a linear relationship between concentrations of BP-AgNPs and percentage inhibition of alpha-amylase. Acarbose is treated as a positive control. The experiment was performed in triplicate and mean \pm SD was calculated. All the values are statistically significant ($p < 0.05$).

Table 3. Values represented in (Mean \pm SD) and significant level ($p < 0.05$), through one-way ANOVA of alpha-amylase assay.

Concentrations ($\mu\text{g/mL}$)	Mean \pm SD (AgNPs)	Mean \pm SD (Acarbose)
25	0.34 \pm 0.034	0.43 \pm 0.01
50	0.32 \pm 0.036	0.35 \pm 0.01
75	0.32 \pm 0.03	0.32 \pm 0.032
100	0.27 \pm 0.01	0.22 \pm 0.05
125	0.20 \pm 0.10	0.14 \pm 0.01

3.3.3. Inhibition of Protein Denaturation by BP-AgNPs

Silver nanoparticles were found to inhibit the denaturation of albumin through heat. On heating, AgNPs containing the reaction mixture had no cloudy appearance and precipitation, while the egg albumin without AgNPs on heating turned into white precipitation. The inhibition increased with the increase in the concentration of AgNPs. The maximum inhibition was 81.13% at 500 $\mu\text{g/mL}$, more than that of the reference drug diclofenac sodium, which shows 73.58% at the same concentration (Figure 9). The significant values has been shown in Table 4.

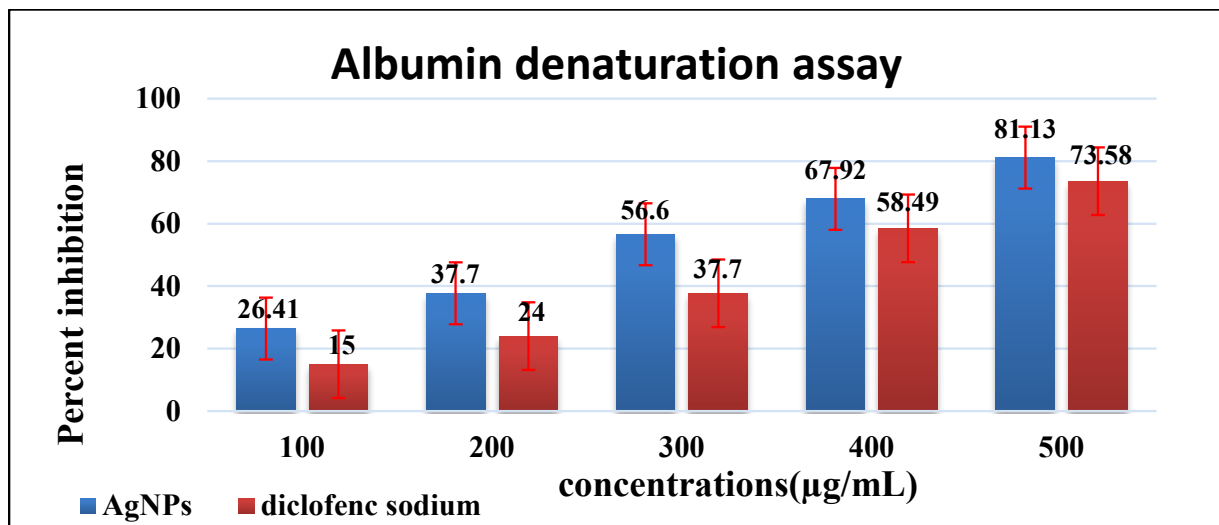


Figure 9. Graphical representation of percentage inhibition of albumin denaturation by BP-AgNPs and standard drug diclofenac sodium. Values are represented in (Mean \pm SD) and significant level ($p < 0.05$), through one-way ANOVA.

Table 4. Values represented in (Mean \pm SD) and significant level ($p < 0.05$), through one-way ANOVA of protein denaturation assay.

Concentrations ($\mu\text{g/mL}$)	(Mean \pm SD) (AgNPs)	(Mean \pm SD) (Diclofenac Sodium)
100	0.39 \pm 0.00	0.45 \pm 0.15
200	0.33 \pm 0.005	0.40 \pm 0.10
300	0.24 \pm 0.017	0.32 \pm 0.032
400	0.17 \pm 0.010	0.22 \pm 0.05
500	0.1 \pm 0.00	0.14 \pm 0.01

3.3.4. Cytotoxic Activity of AgNPs (MTT Assay)

Cytotoxic assays on U87 and HEK 293 cell lines demonstrate toxic effects on cell viability. With the increase in concentration, the percentage of cell viability decreases (Figure 10). The orange bodies in (Table 5) are indicated as dead cells as well as cell morphology changes in a concentration-dependent manner. The IC_{50} values for U87 (Figure 10A) and HEK 293 (Figure 10B) cell lines after 24 and 48 h of exposure are (164.85 $\mu\text{g/mL}$, 150.38 $\mu\text{g/mL}$) and (168.97 $\mu\text{g/mL}$, 167.79 $\mu\text{g/mL}$), respectively (Table 6).

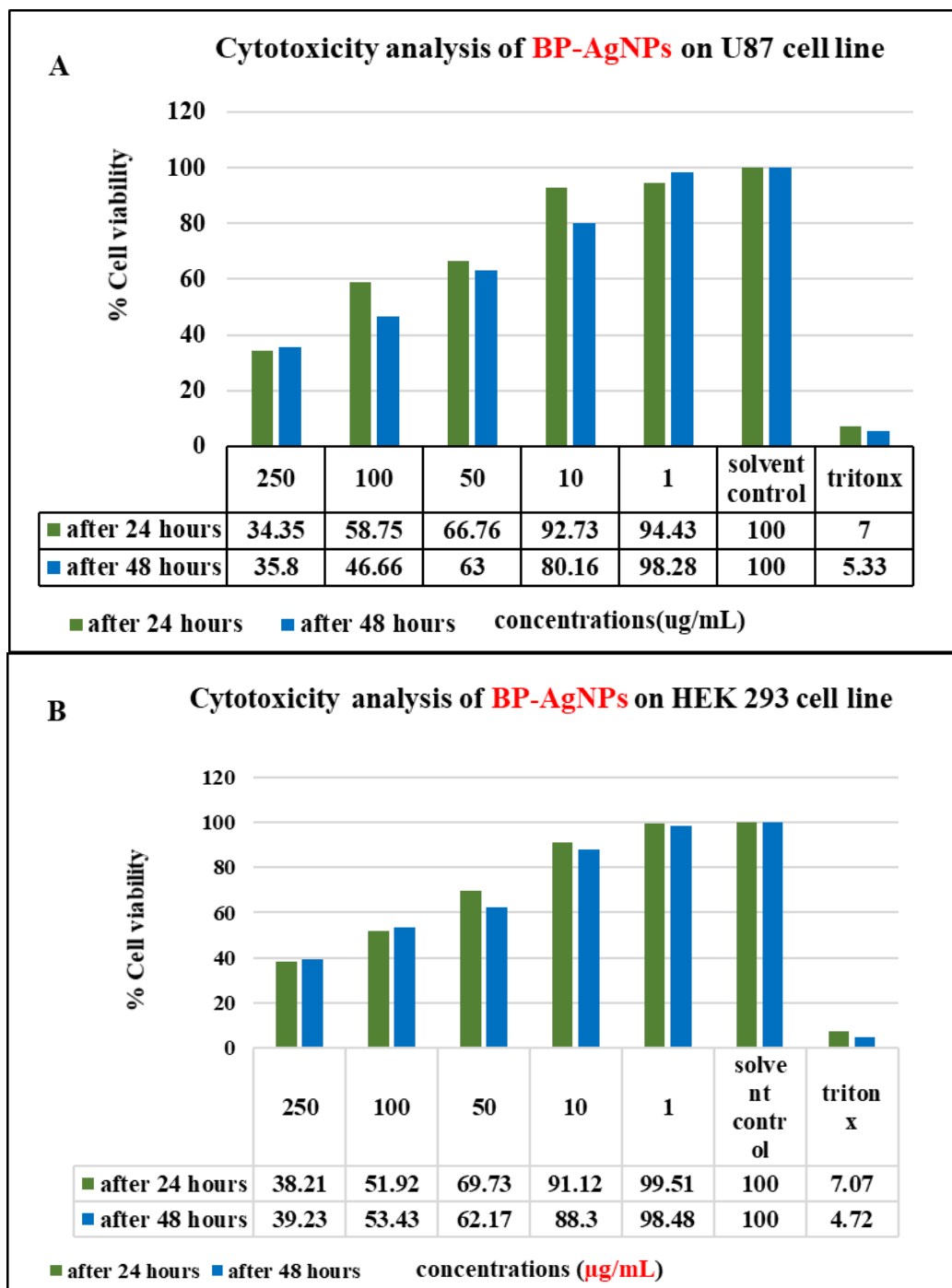


Figure 10. Cytotoxic potency of silver nanoparticles on cancer cell line (A) U87 and (B) HEK293 after 24 and 48 h of exposure.

Table 5. Effect of biosynthesized silver nanoparticles on cell morphology of U87 and HEK293 cell lines.

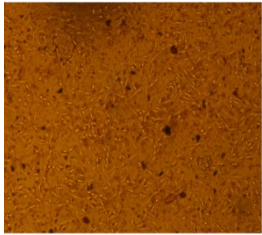
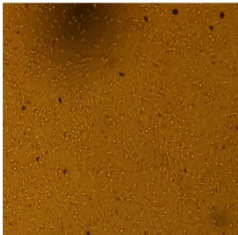
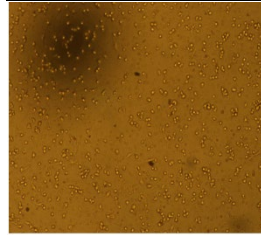
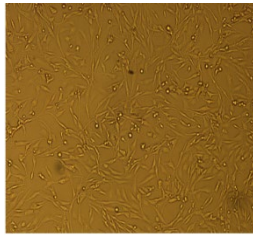
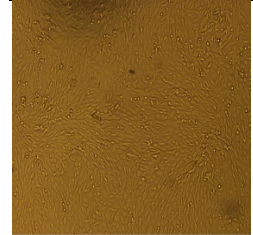
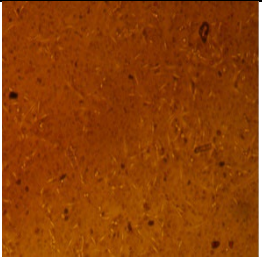

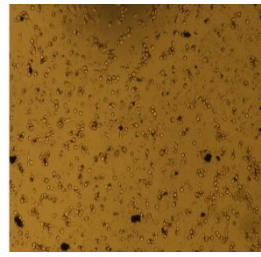
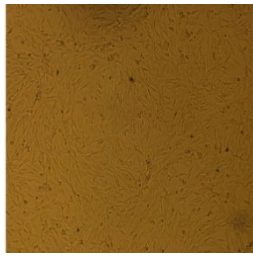
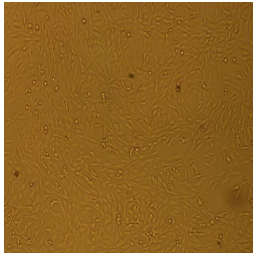

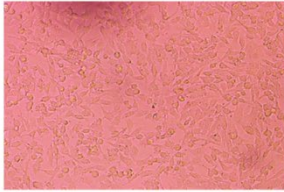
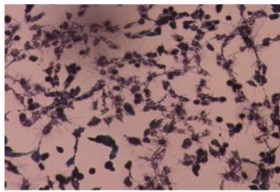
Cell Lines	Concentrations ($\mu\text{g/mL}$) of (BP-AgNPs)				
	250	100	50	10	1
HEK Cell Line					
U87-MG Cell Line					
					
	Positive control	Solvent control	MTT treated cells		

Table 6. Minimum inhibitory concentration IC₅₀ values for DPPH, alpha-amylase and MTT assay.

DPPH Assay IC ₅₀		Alpha-Amylase Assay IC ₅₀		MTT Assay IC ₅₀	
BP-AgNPs	Ascorbic acid	BP-AgNPs	Acarbose	U87 after 24 and 48 h)	HEK293 (after 24 and 48 h)
33.85 µg/mL	50 µg/mL	67 µg/mL	110 µg/mL	164.85 µg/mL, 150.38 µg/mL	168.97 µg/mL, 167.79 µg/mL

4. Discussion

Physiochemical manufacturing techniques are frequently abandoned in the preparation of nanoparticles because of their use of hazardous substances and toxic residues that disturb the atmosphere, and they are also expensive, making them unsuitable for the clinical field. Due to their excellent optoelectronic, catalytic, magnetic, and harmless characteristics, as well as their eco-sustainable attitude and adaptability in biomedicine, the green synthesis of metallic nanoparticles has created a curiosity in nanotechnology studies [25–27]. Keeping all this in mind, the current study reported plant extract-mediated green synthesis of silver nanoparticles. Synthesis of nanoparticles using biological means, i.e., by the leaf extract of the *Brachyhiton populneus* plant, is biocompatible due to the secretion of functional biomolecules such as alkaloids, flavonoids, sterols etc. which actively reduce metal ions as compared with the synthesis of nanoparticles with the assistance of other biomaterials such as various polymers which are less efficient and not cost-effective. The *Brachyhiton populneus* leaf extract reacts with silver nitrate solution and changes from a yellow color to a brown suspension by reducing Ag⁺ ions to Ag⁰, confirmatory results can be found in [28]. According to Khalil et al. [29], BP-AgNPs may show a surface plasmon resonance spectrum of 440–558 nm. In a previously reported study by Das et al. [30], silver nanoparticles exhibit absorbance peaks at 458 and 446 nm.

In the present work, the maximum absorbance peak occurred at 453 nm due to the surface plasmon resonance property. The outcomes suggest that phytoconstituents in the extract act as reducing and capping agents. Further, the morphology and size of silver nanoparticles were predicted by scanning electron microscopy (SEM), which revealed a cubical shape as in Ibrahim et al. [31]. In the current study, the histogram displayed particle size distribution within the range of 10–50 nm, with the average particle size calculated by ImageJ software as 12 nm. According to Aslam et al. [32], the histogram depicts the average particle size distribution as between 10–80 nm. The energy dispersive X-ray (EDX) analysis predicted an elemental composition of silver nanoparticles that demonstrated the presence of chlorine, oxygen, and silver. The higher values of Ag indicate the existence of silver nanoparticles [32]. The effective stability of silver nanoparticles by phytoconstituents on particle surfaces was predicted by FTIR measurements. The nanoparticles conjugated with alkane (O–H), alcohol (C–H), fluoro (C–F), nitro (C–N), carboxyl, amine, alkenes (C=C), phenol (O–H), sulfone (S–O) and halo compound (C–Cl) were in accordance with that previously reported by [30,33].

The antioxidant and antidiabetic activity of AgNPs was depicted by DPPH reduction and alpha-amylase assay, respectively, as the change in color in the reaction mixture. The % inhibition occurred in a dose-dependent manner as an increase in concentration increased inhibition. The IC₅₀ value of the DPPH assay by AgNPs was 33.85 µg/mL and 67 µg/mL in the amylase assay. Mohanta et al. [28] explored the antioxidant potential of silver nanoparticles synthesized from *Erythrina suberosa* (Roxb.) leaf extract. The IC₅₀ value calculated in the DPPH assay was 30.04 µg/mL which strengthens ongoing research work. The antidiabetic potency of AgNPs was elaborated using *Punica granatum* leaf extract, which exhibited a significant IC₅₀ value of 65.2 µg/mL [34], contemporary to the present study.

Moreover, statistical analysis also explores the significance of data and findings. The ascorbic acid and BP-AgNPs have the capacity to scavenge DPPH at various concentrations. It was shown that there are significant variations in the values of the tested items with a probability of $p < 0.05$. According to Abdellatif et al. [35], BP-AgNPs show a higher

significant difference in protein denaturation assay than AgNPs at $p < 0.01$ while the current study shows significance at $p < 0.05$. Otunola et al. [36] also strengthen the present work by calculating mean values and significant differences at $p < 0.05$. A study on the antidiabetic activity of silver nanoparticles performed by Das et al. [30], found a significant effect ($p < 0.05$) which is in agreement with this study.

The current study demonstrated significant cytotoxicity of BP-AgNPs against cancer cell lines U87 and HEK 293. The % cell viability decreased as the concentration of silver nanoparticles increased. The concentration-dependent anti-proliferative activity of *Pechueloeschia leubnitziae* extract-mediated silver nanoparticles against the U87 glioblastoma cell line proved anticancer potential [37,38]. The cytotoxic effect of *Syzygium cumini*-mediated silver nanoparticles on the HEK 293 cell line shown by Mittal et al. [39] also confirmed the significance of our results. They suggested cell viability depends on dose concentration. The current first-ever biosynthesis of nanoparticles from *Brachychiton populneus* leaf extract has astonishing biological properties that explore the effectiveness of green synthesis in the nanotechnology field.

5. Conclusions

The current study explored the one-step green synthesis of silver nanoparticles (BP-AgNPs) from *Brachychiton populneus* leaf extract, which may be an eco-friendly, safe, and less-expensive approach. At room temperature, the synthesized nanoparticles have a small size of 12 nm in diameter and a cubical shape, as predicted by the SEM technique. The plant metabolites act as reducing and capping agents in the synthesis process. These metabolites were verified by FTIR measurements as being responsible for nanoparticle synthesis. Furthermore, the synthesized nanoparticles were screened to examine biological properties. These nanoparticles exhibit remarkable in vitro antioxidant, anti-inflammatory, antidiabetic, and cytotoxic potential. The current study concludes that biosynthesized nanoparticles have robust enough attributes to revolutionize biomedical science and can be used as a drug to overcome disorders. *Brachychiton populneus* extract has the potential to produce other metal and metal oxide nanoparticles. Moreover, the plant-mediated fabrication of silver nanoparticles is less energetic, beneficial to living beings, produces minimal waste, and is compatible with the environment.

Author Contributions: Conceptualization, M.N., H.B., S.I.M., A.J. and S.u.R.; Original draft, M.N., H.B., M.Y.S. and T.A.; Methodology, M.N., H.B., S.I.M., A.S.D. and T.A.; Data curation: A.A.M., M.W.A. and A.J.; Writing—review & editing, M.N., H.B. and S.I.M. Visualization, S.u.R., A.J., A.A.A., A.S.A. and M.A.; Resources, M.N., T.A. and A.S.D.; Project administration, M.N., M.W.A. and T.A.; Funding acquisition, A.A.A., A.S.A. and M.A.; Validation, A.A.M., S.u.R., M.A., and A.J.; Investigation, M.N., H.B., S.I.M., T.A. and M.Y.S.; Formal analysis, M.W.A., A.S.D. and S.u.R.; Supervision, M.N. and T.A. All authors have read and agreed to the published version of the manuscript.

Funding: No external funding was received.

Institutional Review Board Statement: Not applicable.

Informed Consent Statement: Not applicable.

Data Availability Statement: All major data generated and analyzed in this study are included in this manuscript and its supplementary information files.

Acknowledgments: A.A.A. would like to acknowledge Taif university for supporting this research article under Taif University Researchers Supporting Project number (TURSP-2020/296), Taif University, Taif, Saudi Arabia.

Conflicts of Interest: The authors declare no conflict of interest.

References

1. Bayda, S.; Adeel, M.; Tuccinardi, T.; Cordani, M.; Rizzolio, F. The History of Nanoscience and Nanotechnology: From Chemical-Physical Applications to Nanomedicine. *Molecules* **2019**, *27*, 112. [[CrossRef](#)]
2. Iqbal, P.; Preece, J.A.; Mendes, P.M. Nanotechnology: The “Top-Down” and “Bottom-Up” Approaches. *Supramol. Chem. Mol. Nanomaterials*. **2012**, *2*, 1–14.
3. Sriramulu, M.; Shanmugam, S.; Ponnusamy, V.K. Agaricus bisporus mediated biosynthesis of copper nanoparticles and its biological effects: An in-vitro study. *Colloids Interface Sci. Commun.* **2020**, *35*, 100254. [[CrossRef](#)]
4. Kuppusamy, P.; Yusoff, M.M.; Maniam, G.P.; Govindan, N. Biosynthesis of metallic nanoparticles using plant derivatives and their new avenues in pharmacological applications—An updated report. *Saudi Pharm. J.* **2016**, *24*, 473–484. [[CrossRef](#)] [[PubMed](#)]
5. Arif, R.; Uddin, R. A review on recent developments in the biosynthesis of silver nanoparticles and its biomedical applications. *Med. Devices Sens.* **2021**, *4*, e10158. [[CrossRef](#)]
6. Shanmuganathan, R.; Karuppusamy, I.; Saravanan, M.; Muthukumar, H.; Ponnuchamy, K.; Ramkumar, V.S.; Pugazhendhi, A. Synthesis of Silver Nanoparticles, and their Biomedical Applications—A Comprehensive Review. *Curr. Pharm. Des.* **2019**, *25*, 2650–2660. [[CrossRef](#)]
7. Jouyban, A.; Rahimpour, E. Optical sensors based on silver nanoparticles for determination of pharmaceuticals: An overview of advances in the last decade. *Talanta* **2020**, *217*, 121071. [[CrossRef](#)]
8. Zeid, A.H.A.; Farag, M.A.; Hamed, M.A.A.; Kandil, Z.A.A.; El-Akad, R.H.; El-Rafie, H.M. Flavonoid chemical composition and antidiabetic potential of *Brachychiton acerifolius* leaves extract. *Asian Pac. J. Trop. Biomed.* **2017**, *7*, 389–396. [[CrossRef](#)]
9. Ragheb, A.Y.; Kassem, E.S.; El-Sherei, M.; Marzouk, M.; Saleh, A.M.; Saleh, N.A.M. Morphological, phytochemical, and anti-hyperglycemic evaluation of *Brachychiton populneus*. *Rev. Bras. Farmacogn.* **2019**, *29*, 559–569. [[CrossRef](#)]
10. Agyare, C.; Koffuor, G.A.; Boamah, V.E.; Adu, F.; Mensah, K.B.; Adu-Amoah, L. Antimicrobial and Anti-Inflammatory Activities of *Pterygota macrocarpa* and *Cola gigantea* (Sterculiaceae). *Evid Based Complement. Altern. Med.* **2012**, *2012*, 902394. [[CrossRef](#)]
11. Aadil, K.R.; Pandey, N.; Mussatto, S.I.; Jha, H. Green synthesis of silver nanoparticles using acacia lignin, their cytotoxicity, catalytic, metal ion sensing capability and antibacterial activity. *J. Environ. Chem. Eng.* **2019**, *7*, 103296. [[CrossRef](#)]
12. Agarwal, H.; Nakara, A.; Shanmugam, V.K. Anti-inflammatory mechanism of various metal and metal oxide nanoparticles synthesized using plant extracts: A review. *Biomed. Pharmacother.* **2019**, *109*, 2561–2572. [[CrossRef](#)] [[PubMed](#)]
13. Murugesan, K.; Koroth, J.; Srinivasan, P.P.; Singh, A.; Mukundan, S.; Karki, S.S.; Choudhary, B.; Gupta, C.M. Effects of green synthesised silver nanoparticles (ST06-AgNPs) using curcumin derivative (ST06) on human cervical cancer cells (HeLa) in vitro and EAC tumor bearing mice models. *Int. J. Nanomed.* **2019**, *16*, 5257–5270. [[CrossRef](#)]
14. Gurunathan, S.; Han, J.W.; Eppakayala, V.; Jeyaraj, M.; Kim, J.H. Cytotoxicity of biologically synthesized silver nanoparticles in MDA-MB-231 human breast cancer cells. *Biomed. Res. Int.* **2013**, *2013*, 535796. [[CrossRef](#)]
15. Darvish, S.; Kahrizi, M.S.; Özbolat, G.; Khaleghi, F.; Mortezania, Z.; Sakhaei, D. Silver nanoparticles: Biosynthesis and cytotoxic performance against breast cancer MCF-7 and MDA-MB-231 cell lines. *Nanomed. Res. J.* **2022**, *7*, 83–92.
16. Bhardwaj, M.; Yadav, P.; Dalal, S.; Kataria, S.K. A review on ameliorative green nanotechnological approaches in diabetes management. *Biomed. Pharm.* **2020**, *127*, 110198. [[CrossRef](#)]
17. Akhtar, M.J.; Ahamed, M.; Alhadlaq, H.A.; Alshamsan, A. Mechanism of ROS scavenging and antioxidant signalling by redox metallic and fullerene nanomaterials: Potential implications in ROS associated degenerative disorders. *Biochim. Biophys Acta Gen. Subj.* **2017**, *1861*, 802–813. [[CrossRef](#)]
18. Mohammad, G.; Mishra, V.K.; Pandey, H.P. Antioxidant properties of some nanoparticles may enhance wound healing in T2DM patient. *Dig. J. Nanomater. Biostructures* **2008**, *3*, 159–162.
19. Lushchak, O.; Zayachkivska, A.; Vaiserman, A. Metallic Nanoantioxidants as Potential Therapeutics for Type 2 Diabetes: A Hypothetical Background and Translational Perspectives. *Oxid Med. Cell Longev.* **2018**, *2018*, 27. [[CrossRef](#)]
20. Zhang, W.; Chen, L.; Xiong, Y.; Panayi, A.C.; Abududilibaier, A.; Hu, Y.; Yu, C.; Zhou, W.; Sun, Y.; Liu, M.; et al. Antioxidant Therapy and Antioxidant-Related Bionanomaterials in Diabetic Wound Healing. *Front. Bioeng. Biotechnol.* **2021**, *24*, 707479. [[CrossRef](#)]
21. Bawazeer, S.; Rauf, A.; Shah, S.U.A.; Shawky, A.M.; Al-Awthan, Y.S.; Bahattab, O.S.; Uddin, G.; Sabir, J.; El-Esawi, M.A. Green synthesis of silver nanoparticles using *Tropaeolum majus*: Phytochemical screening and antibacterial studies. *Green Proc. Synth.* **2021**, *10*, 85–94. [[CrossRef](#)]
22. Braca, A.; de Tommasi, N.; di Bari, L.; Pizza, C.; Politi, M.; Morelli, I. Antioxidant Principles from *Bauhinia tarapotensis*. *J. Nat. Prod.* **2001**, *64*, 892–895. [[CrossRef](#)] [[PubMed](#)]
23. Xiong, Y.; Ng, K.; Zhang, P.; Warner, R.D.; Shen, S.; Tang, H.Y.; Liang, Z.; Fang, Z. In Vitro α -Glucosidase and α -Amylase Inhibitory Activities of Free and Bound Phenolic Extracts from the Bran and Kernel Fractions of Five Sorghum Grain Genotypes. *Foods* **2020**, *15*, 1301. [[CrossRef](#)] [[PubMed](#)]
24. Anwar, S.; Almatroudi, A.; Allemailem, K.S.; Jacob Joseph, R.; Khan, A.A.; Rahmani, A.H. Protective Effects of Ginger Extract against Glycation and Oxidative Stress-Induced Health Complications: An In Vitro Study. *Processes* **2020**, *8*, 468. [[CrossRef](#)]
25. Nguyen, N.H.A.; Padil, V.V.T.; Slaveykova, V.I.; Černík, M.; Ševců, A. Green Synthesis of Metal and Metal Oxide Nanoparticles and Their Effect on the Unicellular Alga *Chlamydomonas reinhardtii*. *Nanoscale Res. Lett.* **2018**, *13*, 159. [[CrossRef](#)] [[PubMed](#)]
26. Sharma, D.; Kanchi, S.; Bisetty, K. Biogenic synthesis of nanoparticles: A review. *Arab. J. Chem.* **2019**, *12*, 3576–3600. [[CrossRef](#)]

27. Patil, S.; Chandrasekaran, R. Biogenic nanoparticles: A comprehensive perspective in synthesis, characterization, application, and its challenges. *J. Genet. Eng. Biotechnol.* **2020**, *18*, 67. [[CrossRef](#)] [[PubMed](#)]
28. Mohanta, Y.K.; Panda, S.K.; Jayabalan, R.; Sharma, N.; Bastia, A.K.; Mohanta, T.K. Antimicrobial, Antioxidant and Cytotoxic Activity of Silver Nanoparticles Synthesized by Leaf Extract of *Erythrina suberosa* (Roxb.). *Front. Mol. Biosci.* **2017**, *17*, 14. [[CrossRef](#)] [[PubMed](#)]
29. Khalil, M.M.H.; Ismail, E.H.; El-Baghdady, K.Z.; Mohamed, D. Green synthesis of silver nanoparticles using olive leaf extract and its antibacterial activity. *Arab. J. Chem.* **2014**, *7*, 1131–1139. [[CrossRef](#)]
30. Das, G.; Patra, J.K.; Debnath, T.; Ansari, A.; Shin, H.S. Investigation of antioxidant, antibacterial, antidiabetic, and cytotoxicity potential of silver nanoparticles synthesized using the outer peel extract of *Ananas comosus* (L.). *PLoS ONE* **2019**, *12*, e0220950. [[CrossRef](#)]
31. Ibrahim, E.H.; Kilany, M.; Ghramh, H.A.; Khan, K.A.; Ul Islam, S. Cellular proliferation/cytotoxicity, and antimicrobial potentials of green synthesized silver nanoparticles (AgNPs) using *Juniperus procera*. *Saudi J. Biol. Sci.* **2019**, *26*, 1689–1694. [[CrossRef](#)]
32. Aslam, M.; Fozia, F.; Gul, A.; Ahmad, I.; Ullah, R.; Bari, A.; Mothana, R.A.; Hussain, H. Phyto-Extract-Mediated Synthesis of Silver Nanoparticles Using Aqueous Extract of *Sanvitalia procumbens* and Characterization, Optimization and Photocatalytic Degradation of Azo Dyes Orange G and Direct Blue-15. *Molecules* **2021**, *12*, 6144. [[CrossRef](#)] [[PubMed](#)]
33. Krithiga, N.; Rajalakshmi, A.; Jayachitra, A. Green Synthesis of Silver Nanoparticles Using Leaf Extracts of *Clitoria ternatea* and *Solanum nigrum* and Study of Its Antibacterial Effect against Common Nosocomial Pathogens. *J. Nanosci.* **2015**, *2015*, 928204. [[CrossRef](#)]
34. Saratale, R.G.; Shin, H.S.; Kumar, G.; Benelli, G.; Kim, D.S.; Saratale, G.D. Exploiting antidiabetic activity of silver nanoparticles synthesized using *Punica granatum* leaves and anticancer potential against human liver cancer cells (HepG2). *Artif. Cells Nanomed. Biotechnol.* **2018**, *46*, 211–222. [[CrossRef](#)]
35. Abdellatif, A.A.H.; Alhathloul, S.S.; Aljohani, A.S.M.; Maswadeh, H.; Abdallah, E.M.; Musa, K.H.; el Hamd, M.A. Green Synthesis of Silver Nanoparticles Incorporated Aromatherapies Utilized for Their Antioxidant and Antimicrobial Activities against Some Clinical Bacterial Isolates. *Bioinorg. Chem. Appl.* **2022**, *2022*, 2432758. [[CrossRef](#)] [[PubMed](#)]
36. Otunola, G.A.; Afolayan, A.J. Chemical Composition, Antibacterial and in vitro Anti-Inflammatory Potentials of Essential Oils from Different Plant Parts of *Moringa oleifera* Lam. *Am. J. Biochem. Biotechnol.* **2018**, *14*, 210–220. [[CrossRef](#)]
37. Mofolo, M.J.; Kadhila, P.; Chinsebu, K.C.; Mashele, S.; Sekhoacha, M. Green synthesis of silver nanoparticles from extracts of *Pechuel-oeschea leubnitziae*: Their anti-proliferative activity against the U87 cell line. *Inorg. Nano-Met. Chem.* **2020**, *50*, 949–955. [[CrossRef](#)]
38. Algebaly, A.S.; Mohammed, A.E.; Abutaha, N.; Elobeid, M.M. Biogenic synthesis of silver nanoparticles: Antibacterial and cytotoxic potential. *Saudi J. Biol. Sci.* **2020**, *27*, 1340–1351. [[CrossRef](#)]
39. Mittal, A.K.; Thanki, K.; Jain, S.; Banerjee, U.C. Comparative studies of anticancer and antimicrobial potential of bioinspired silver and silver-selenium nanoparticles. *J. Mater. Nanosci.* **2016**, *3*, 22–27.